Fibers and Polymers (2024) 25:1349–1366
https://doi.org/10.1007/s12221-024-00507-6

Online ISSN 1875-0052
Print ISSN 1229-9197

REGULAR ARTICLE

Design, Synthesis, Characterization, and Antimicrobial Properties of New Azo Disperse Dyes Incorporating Quinazolinone-Pyrazolone Moieties and Their Applications for Dyeing of Polyester Fabrics

Seham A. Ibrahim[1] · Adel I. Selim[1] · Asmaa M. Sakr[1] · Safia A. Mahmoud[2] · Ahmed A. Noser[1]

Received: 16 October 2023 / Revised: 30 November 2023 / Accepted: 18 February 2024 / Published online: 14 March 2024

Abstract
The current study outlines a straightforward and efficient method for creating new quinazolinone disperse dyes based on pyrazolone moieties, starting with quinazolinone and a variety of substituted pyrazolone as couplers. The synthesized dyes were characterized using a variety of spectroscopic and analytical methods. The synthesized dyes' ultraviolet–visible spectra showed bands brought on by several molecular transitions. We investigated in detail the multifunctional characteristics such color representation, dyeing duration, concentration, pH, buildup, and fastness properties of the dyed samples. Fastness properties and colorimetric data showed satisfactory results, demonstrating the effectiveness of these dyes in dyeing polyester fabrics. A pH of 5 and a dyeing temperature of 130 °C were the ideal conditions for dyeing polyester fabrics. Additionally, an ultraviolet protection factor test was performed on the dyed fabrics, and the results showed that these dyes provide the best UV protection. These dyes are suitable for industrial dyeing applications since they are easy to manufacture and scale up. Additionally, *in-vitro* testing was done to determine the dyes' antibacterial effectiveness against various bacteria and fungi. The antibacterial activity of the dyes was moderate to very good against both Gram-positive and Gram-negative bacteria, as well as fungi.

Keywords Quinazolinone · Pyrazolone · Disperse dyes · Fastness · Ultraviolet protection · Antimicrobial activity

1 Introduction

Because of its excellent physical properties, process ability, lower price, superior mechanical properties, high strength, wear resistance, and other attributes, polyester, specifically polyethylene terephthalate (PET), is the most widely used material in the apparel and textiles industry[1, 2].

Due to their extensive application in industry and science, azo dyes are a crucial class of colorant chemicals [3]. Azo dyes are the most widely used synthetic dyes because they are simple to synthesis and have a variety of commercial uses, such as paper printing, cosmetics, plastic, polymer coloring, and textile dyeing [4, 5], as well as advanced applications in organic synthesis [6–8]. They have found use in the pharmaceutical and biological industries [9–11] as their anti-inflammatory [12, 13], anticancer [14, 15], antibacterial [16–18], and antifungal [19, 20] properties as well as their use in protein synthesis, DNA/RNA inhibition, and nitrogen fixation [21]. Additionally, because of their affordability, simplicity of synthesis, stability, and range of colors, azo dye synthesized is superior to that of natural dyes in the dyestuff industry. It is well known that azo dyes with a heterocyclic moiety have certain characteristics, including high coloring power, high tinctorial strength, fastness, and high thermal stability. Moreover, azo dyes have a stronger cell bathochromic effect than dyes with simple aromatic systems [22–25].

Pyrazole and its derivatives have a wide range of applications in the fields of materials science, dyes, agrochemicals, and medicine [26]. Pyrazolone derivatives' broad range of pharmacological characteristics, which include antimicrobial, antitumor, CNS activity, anti-inflammatory, antioxidant,

✉ Seham A. Ibrahim
seham.ibrahim@science.tanta.edu.eg;
sehamabdelatif@yahoo.com

✉ Ahmed A. Noser
ahmed.nosir@science.tanta.edu.eg

[1] Chemistry Department, Faculty of Science, Tanta University, Tanta 31527, Egypt

[2] Textile Industries Research Division, Dyeing Printing and Textile Auxiliaries Department, National Research Centre, 33-El_Behouth St.,Dokki, P.O.12622, Giza, Egypt

anti-tubercular, antiviral, lipid-lowering, antihyperglycemic, and protein inhibitory activities, have been documented [27, 28]. These days, a number of FDA-approved drugs with pyrazolone nucleus have been investigated (Fig. 1). Examples of these include metamizole, edaravone, aminophenazone, eltrombopag, and dichloralphenazone. A number of pyrazolone-containing investigational small molecules, such as sulfamazone, propyphenazone, and nifenazone [29] have been considered as potential drugs.

Quinazolinone derivatives, a significant class of alkaloids, have demonstrated a wide range of biological properties, including anti-cancer, antiviral, antibacterial, and antiparkinsonism [30–32]. This suggests that quinazolinone derivatives are more biocompatible, which is a benefit when considering them as potential fluorophores in biological research.

In comparison to azo dyes synthesis from a simple aromatic amine, azo dyes integrating heterocyclic moieties show improved coloring capabilities, tinctorial strength, thermal stability, and more favorable solvatochromic behavior [33, 34].These dyes are also utilized as chemotherapeutic and antibacterial agents to stain and paralyze particular microorganisms [35]. Azo dyes with enhanced dyeing and outstanding pharmacological activities were reported earlier by different researchers and produced from pyrazolone and quinazolinone moieties, it has been demonstrated that dyes-based materials have good fastness and stability characteristics [36–39]. Fabric strength and quality decline as well as odors, discoloration, and health problems are all brought on by microbes such bacteria, fungi, and mildew [40, 41]. To prevent bacterial growth in fabrics, antibacterial fabrics were created and are now utilized in diverse environments, including the medical industry and daily life [42].

As a part of our continuous interest on synthesis of new heterocyclic dyes [43–47], the goal of this study is to synthesize a series of new disperse quinazolinone dyes based on pyrazolone derivatives and study their applications as disperse dyes to polyester fabrics, Color representation, colorimetric data, UV protection and multifunctional features have also been studied. In addition, the synthetic dyes were tested *in-vitro* against different bacteria and fungi. Numerous studies demonstrated the outstanding characteristics of quinazolinone-pyrazolone monoazo dyes. When the new quinazolinone-pyrazolone dyes are compared to some of the previously published dyes [48, 49], the results indicate that the published dyes primarily yellow and light-yellow shades, whereas the new dyes deeper shades. Furthermore, it was found that the percentage of dye bath exhaustion on polyester fabrics was acceptable and fairly good, whereas the exhaustion of new dyes is excellent. The light fastness of dyed fibers is fair to good, whereas that of new dyes is good to very good.

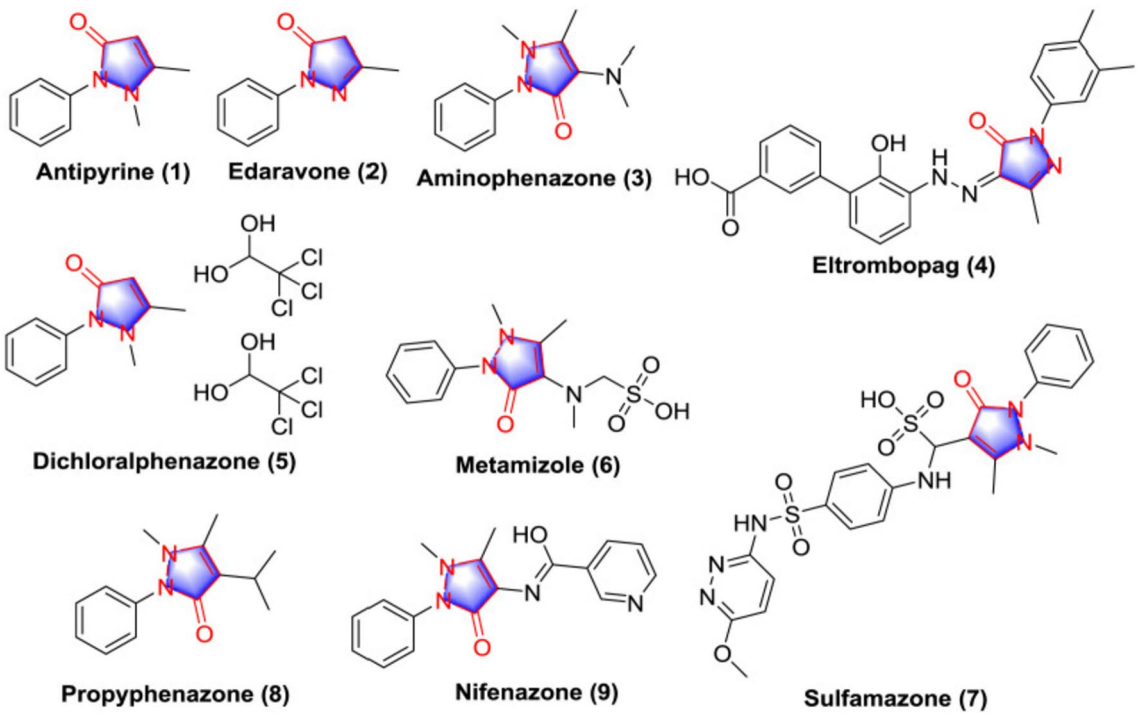

Fig. 1 Drugs containing pyrazolone as a bioactive heterocyclic pharmacophore

2 Experimental Sections

2.1 Instrumentation of Spectral Analyses and Melting Points

All data on chemicals and instruments are available in the supplementary file **(Section S1).**

2.2 General Method for the Synthesis of Compound 2 and 3

4-Amino acetophenone (1.35 g, 10 mmol) was refluxed for 6 h (TLC control) with an ethanolic solution of compound **1a** or **1b** (10 mmol) in a few drops of acetic acid. The reaction mixture was then added to ice water, filtered, and dried.

3-(4-((1-(4-aminophenyl)ethylidene)amino)phenyl)-2-phenylquinazolin-4(3H)-one **(2)**

MP. 85–87 °C; **yield**: 88%; **IR** (KBr) ν: 3412 (NH_2), 3066 (CH-arom), 2923 (CH-aliph), 1735 (CO), 1622 (C = N); **^{1}H-NMR** (400 MHz, DMSO-d_6) δ 12.21 (s, 2H, NH_2), 6.51–8.69 (m, 17H, Ar–H), 2.34 (s, 3H, CH_3); **^{13}C-NMR** (101 MHz, DMSO-d_6) δ 170.58 (C = N schiff base), 165.23 (C = O quinazolinone), 154.03 (C = N quinazolinone), 141.66 (C-NH_2), 113.02–135.11 (Ar–C), 26.32 (CH_3); **Anal.** Calcd for $C_{28}H_{22}N_4O$ (430.51) C, 78.12%; H, 5.15%; N, 13.01%; Found: C, 77.96%; H, 5.03%; N, 12.91%.

3-((1-(4-aminophenyl)ethylidene)amino)-2-phenylquinazolin-4(3H)-one **(3)**

MP. 150–152 °C; **yield**: 87%; **IR** (KBr) ν: 3422 (NH_2), 3026 (CH-arom), 2942 (CH-aliph), 1765 (CO), 1625 (C = N); **^{1}H-NMR** (400 MHz, DMSO-d_6) δ 12.15 (s, 2H, NH_2), 7.17–8.69 (m, 13H, Ar–H), 2.25 (s, 3H, CH_3); **^{13}C-NMR** (101 MHz, DMSO-d_6) δ 170.54 (C = N schiff base), 165.23 (C = O quinazolinone), 159.52 (C = N quinazolinone), 141.67 (C-NH_2), 117.08–135.09 (Ar–C), 29.31 (CH_3); **Anal**. Calcd for $C_{22}H_{18}N_4O$ (354.41) C, 74.56%; H, 5.12%; N, 15.81%; Found: C, 74.36%; H, 5.02%; N, 15.61%.

2.3 General Method for the Synthesis of Quinazolinone Azo Compounds 4a-e and 5a-e

A cooled solution of sodium nitrite (0.9 g, 12.7 mmol) in water was added dropwise to a cooled solution of compounds **2** and/or **3** (13.7 mmol) in concentrated HCl. The diazonium salt was then dropped into a cooled mixture of various pyrazolone derivatives (8.5 mmol) in pyridine (10 ml). The reaction mixture was stirred overnight at 0 °C, the product was filtered, crystallized from ethanol, and drying it to produced compounds **4a-e and 5a-e**.

3-(4-(((Z)-1-(4-((E)-(1-(2,4-dinitrophenyl)-5-oxo-3-phenyl-4,5-dihydro-1H-pyrazol-4-yl)diazenyl) phenyl) ethylidene)amino) phenyl)-2-phenylquinazolin-4(3H)-one **(4a)**

MP. 138–140 °C; **yield**: 84%; **IR** (KBr) ν: 3029 (CH-arom), 2925 (CH-aliph), 1681(CO), 1644 (C = N), 1598 (N = N); **^{1}H-NMR** (400 MHz, DMSO-d_6) δ 12.14 (s,1H,OH or NH), 7.55–8.68 (m, 25H, Ar–H), 6.07 (s, 1H, CH-pyrazolone), 2.34 (s, 3H, CH_3); **^{13}C-NMR** (101 MHz, DMSO-d_6) δ 170.51 (C = N schiff base), 165.25 (C = O pyrazolone), 163.10 (C = O quinazolinone), 155.50 (C = N quinazolinone), 145.00 (C = N pyrazolone), 120.45–141.65 (Ar–C), 94.75 (CH pyrazolone), 27.21(CH_3); **Anal**. Calcd for $C_{43}H_{29}N_9O_6$ (767.22) C, 67.27%; H, 3.81%; N, 16.42%; Found: C, 67.13%; H, 3.63%; N, 16.28%.

3-(4-(((Z)-1-(4-((E)-(5-oxo-3-(pyridin-3-yl)-4,5-dihydro-1H-pyrazol-4-yl)diazenyl) phenyl) ethylidene) amino) phenyl)-2-phenylquinazolin-4(3H)-one **(4b)**

MP. 230–232 °C; **yield**: 86%; IR (KBr) ν: 3424 (NH), 3023 (CH-arom), 2923 (CH-aliph), 1711 (CO), 1665 (C = N), 1552 (N = N); **^{1}H-NMR** (400 MHz, DMSO-d_6) δ 12.37 (s,1H,OH or NH), 12.05 (s, 1H, NH), 7.61–9.19 (m, 21H, Ar–H), 6.08 (s, 1H, CH-pyrazolone), 2.46 (s, 3H, CH_3); **^{13}C-NMR** (101 MHz, DMSO-d_6) δ 160.51 (C = N Schiff base), 155.50 (C = O pyrazolone), 154.10 (C = O quinazolinone), 149.22 (C = N quinazolinone), 148.79 (C = N pyrazolone), 116.37–146.11 (Ar–C), 81.95 (CH pyrazolone), 27.07 (CH_3); **Anal**. Calcd for $C_{36}H_{26}N_8O_2$ (602.66) C, 71.75%; H, 4.35%; N, 18.59%; Found: C, 71.65%; H, 4.23%; N, 18.39%.

3-(4-(((Z)-1-(4-((E)-(1-(2,4-dinitrophenyl)-5-oxo-3-(pyridin-3-yl)-4,5-dihydro-1H-pyrazol-4-yl)diazenyl) phenyl)ethylidene)amino)phenyl)-2-phenylquinazolin-4(3H)-one **(4c)**

MP.140–142 °C; **yield**: 85%; **IR** (KBr) ν: 3033 (CH-arom), 2927 (CH-aliph), 1745 (CO), 1679 (C = N), 1609 (N = N); **^{1}H-NMR** (400 MHz, DMSO-d_6) δ 12.16 (s,1H,OH or NH), 7.17–8.68 (m, 24H, Ar–H), 6.14 (s, 1H, CH-pyrazolone), 2.42 (s, 3H, CH_3); **^{13}C-NMR** (101 MHz, DMSO-d_6) δ 170.52 (C = N Schiff base), 165.22 (C = O pyrazolone), 160.04 (C = O quinazolinone), 152.84 (C = N quinazolinone), 141.65 (C = N pyrazolone), 117.13–135.08 (Ar–C), 100.01 (CH pyrazolone), 14.01 (CH_3); **Anal**. Calcd for $C_{42}H_{28}N_{10}O_6$ (768.75) C, 65.62%; H, 3.67%; N, 18.22%; Found: C, 65.39%; H, 3.47%; N, 18.12%.

3-(4-(((Z)-1-(4-((E)-(5-oxo-1-phenyl-3-(pyridin-3-yl)-4,5-dihydro-1H-pyrazol-4-yl)diazenyl) phenyl)ethylidene) amino)phenyl)-2-phenylquinazolin-4(3H)-one **(4d)**

MP. 180–182 oC; yeld: 87%; **IR** (KBr) ν: 3068 (CH-arom), 2850 (CH-aliph), 1667 (CO), 1598 (C = N), 1550 (N = N); **^{1}H-NMR** (400 MHz, DMSO-d_6) δ 12.13 (s,1H,OH or NH), 7.46–8.88 (m, 26H, Ar–H), 6.18 (s, 1H, CH-pyrazolone), 2.46 (s, 3H, CH_3); **^{13}C-NMR** (101 MHz,

DMSO-d_6) δ 178.01 (C = N Schiff base), 173.01 (C = O pyrazolone), 165.84 (C = O quinazolinone), 156.90 (C = N quinazolinone), 146.25 (C = N pyrazolone), 117.03–142.70 (Ar–C), 81.90 (CH pyrazolone), 27.13 (CH_3); **Anal.** Calcd for $C_{42}H_{30}N_8O_2$ (678.76) C, 74.32%; H, 4.46%; N, 16.51%; Found: C, 74.32%; H, 4.26%; N, 16.43%.

3-(4-(((Z)-1-(4-((E)-(5-oxo-3-(pyridin-3-yl)-1-(2,4,6-trichlorophenyl)-4,5-dihydro-1H-pyrazol-4-yl) diazenyl) phenyl) ethylidene) amino) phenyl)-2-phenylquinazolin-4(3H)-one **(4e)**

MP. 120–122 °C; yield: 83%; **IR** (KBr) ν: 3040 (CH-arom), 2924 (CH-aliph), 1680 (CO), 1646 (C = N), 1598 (N = N); **^{1}H-NMR** (400 MHz, DMSO-d_6) δ 12.14 (s,1H,OH or NH), 7.54–8.89 (m, 23H, Ar–H), 7.20 (s, 1H, CH-pyrazolone), 2.47 (s, 3H, CH_3); **^{13}C-NMR** (101 MHz, DMSO-d_6) δ 170.48 (C = N Schiff base), 165.25 (C = O pyrazolone), 152.00 (C = O quinazolinone), 149.99 (C = N quinazolinone), 146.50 (C = N pyrazolone), 120.43–146.21 (Ar–C), 99.95 (CH pyrazolone), 18.01 (CH_3); **Anal**. Calcd for $C_{42}H_{27}Cl_3N_8O_2$ (782.08) C, 64.50%; H, 3.48%; Cl, 13.60%; N, 14.33%; Found: C, 64.42%; H, 3.32%; Cl, 13.42%; N, 14.17%.

3-(((Z)-1-(4-((E)-(1-(2,4-dinitrophenyl)-5-oxo-3-phenyl-4,5-dihydro-1H-pyrazol-4-yl)diazenyl) phenyl) ethylidene) amino)-2-phenylquinazolin-4(3H)-one **(5a)**

MP. 165 °C; yield: 83%; IR (KBr) ν: 3050 (CH-arom), 2919 (CH-aliph), 1728 (CO), 1666 (C = N), 1595 (N = N); **^{1}H-NMR** (400 MHz, DMSO-d_6) δ 13.43 (s,1H,OH or NH), 7.44–8.32 (m, 21H, Ar–H), 6.53 (s, 1H, CH-pyrazolone), 2.46 (s, 3H, CH_3); **^{13}C-NMR** (101 MHz, DMSO-d_6) δ 178.01 (C = N Schiff base), 171.74 (C = O pyrazolone), 166.95 (C = O quinazolinone), 161.70 (C = N quinazolinone), 156.30 (C = N pyrazolone), 120.57–144.52 (Ar–C), 99.99 (CH pyrazolone), 22.41 (CH_3); **Anal**. Calcd for $C_{37}H_{25}Cl_3N_9O_6$ (691.66): C, 64.25%; H, 3.64%; N, 18.23%. Found: C, 64.15%; H, 3.42%; N, 18.15%.

3-(((Z)-1-(4-((E)-(5-oxo-3-(pyridin-3-yl)-4,5-dihydro-1H-pyrazol-4-yl)diazenyl) phenyl)ethylidene)amino)-2-phenylquinazolin-4(3H)-one **(5b)**

MP. 180–182 °C; yield: 86%; **IR** (KBr) ν: 3429 (NH), 3052 (CH-arom), 2954 (CH-aliph), 1665 (CO), 1598 (C = N), 1556 (N = N); **^{1}H-NMR** (400 MHz, DMSO-d_6) δ 12.52 (s,1H,OH or NH), 12.23 (s, 1H, NH), 7.45–8.82 (m, 17H, Ar–H), 6.60 (s, 1H, CH-pyrazolone), 2.46 (s, 3H, CH_3); **^{13}C-NMR** (101 MHz, DMSO-d_6) δ 167.85 (C = N Schiff base), 161.61 (C = O pyrazolone), 160.42 (C = O quinazolinone), 156.43 (C = N quinazolinone), 147.00 (C = N pyrazolone), 116.60–145.29 (Ar–C), 90.21 (CH pyrazolone), 27.09 (CH_3); **Anal**. Calcd for $C_{30}H_{22}N_8O_2$ (526.569) C, 68.43%; H, 4.21%; N, 21.28%; Found: C, 68.23%; H, 4.13%; N, 21.12%.

3-(((Z)-1-(4-((E)-(1-(2,4-dinitrophenyl)-5-oxo-3-(pyridin-3-yl)-4,5-dihydro-1H-pyrazol-4-yl)diazenyl) phenyl)ethylidene)amino)-2-phenylquinazolin-4(3H)-one **(5c)**

MP. 140–142 °C;Yield 84%; **IR** (KBr) ν: 3088 (CH-arom), 2932 (CH-aliph), 1717 (CO), 1606 (C = N), 1512 (N = N); **^{1}H-NMR** (400 MHz, DMSO-d_6) δ 11.09 (s,1H,OH or NH), 8.21–9.17 (m, 20H, Ar–H), 7.17 (s, 1H, CH-pyrazolone), 242 (s, 3H, CH_3); **^{13}C-NMR** (101 MHz, DMSO-d_6) δ165.89 (C = N Schiff base), 162.28 (C = O pyrazolone), 160.00 (C = O quinazolinone), 155.06 (C = N quinazolinone), 147.26 (C = N pyrazolone), 113.05–134.82 (Ar–C), 80.89 (CH pyrazolone), 27.21 (CH_3); **Anal**. Calcd for $C_{36}H_{24}N_{10}O_6$ (692.65) C, 65.43%; H, 3.49%; N, 20.22%; Found: C, 65.25%; H, 3.37%; N, 20.08%.

3-(((Z)-1-(4-((E)-(5-oxo-1-phenyl-3-(pyridin-3-yl)-4,5-dihydro-1H-pyrazol-4-yl)diazenyl) phenyl)ethylidene) amino)-2-phenylquinazolin-4(3H)-one **(5d)**

MP. 125–127 °C; yield: 84%; IR (KBr) ν: 3062 (CH-arom), 2942 (CH-aliph), 1666 (CO), 1594 (C = N), 1552 (N = N); **^{1}H-NMR** (400 MHz, DMSO-d_6) δ 13.54 (s,1H,OH or NH), 7.44–7.99 (m, 22H, Ar–H), 7.22 (s, 1H, CH-pyrazolone), 2.46 (s, 3H, CH_3); **^{13}C-NMR** (101 MHz, DMSO-d_6) δ 168.41 (C = N Schiff base), 161.69 (C = O pyrazolone), 156.95 (C = O quinazolinone), 156.40 (C = N quinazolinone), 149.89 (C = N pyrazolone), 116.87–147.11 (Ar–C), 74.78 (CH pyrazolone), 27.09 (CH_3); **Anal**. Calcd for $C_{36}H_{26}N_8O_2$ (602.66) C, 71.75%; H, 4.35%; N, 18.59%; Found: C, 71.75%; H, 4.25%; N, 18.47%.

3-(((Z)-1-(4-((E)-(5-oxo-3-(pyridin-3-yl)-1-(2,4,6-trichlorophenyl)-4,5-dihydro-1H-pyrazol-4-yl)diazenyl) phenyl)ethylidene)amino)-2-phenylquinazolin-4(3H)-one **(5e)**

MP. 110–112 °C; yield: 87%; IR (KBr) ν: 3068 (CH-arom), 2925 (CH-aliph), 1666 (CO), 1596 (C = N), 1553 (N = N); **^{1}H-NMR** (400 MHz, DMSO-d_6) δ 9.23 (s,1H,OH or NH), 7.44–8.99 (m, 19H, Ar–H), 6.52 (s, 1H, CH-pyrazolone), 2.46 (s, 3H, CH_3); **^{13}C-NMR** (101 MHz, DMSO-d_6) δ 161.71 (C = N Schiff base), 156.26 (C = O pyrazolone), 155.52 (C = O quinazolinone), 151.29 (C = N quinazolinone), 148.29 (C = N pyrazolone), 126.56–147.25 (Ar–C), 84.30 (CH pyrazolone), 26.35 (CH_3); **Anal**. Calcd for $C_{36}H_{23}Cl_3N_8O_2$ (705.98) C, 61.25%; H, 3.28%; Cl, 15.06%; N, 15.87%; Found: C, 61.13%; H, 3.16%; Cl, 14.92%; N, 15.67%.

2.4 Electronic Spectral Studies

The electronic spectra of the quinazolinone dyes **4a–e and 5a-e** were studied in the UV region at a molar concentration of 1×10^{-5} mol/L in ethanol, benzene, and dimethylformamide (DMF).

2.5 Dyeing Procedure

2.5.1 General Procedure for Dyeing of Polyester Fabric

The polyester fabrics were dyed using the synthetic dyes as reported [50, 51]. Detailed information about the procedure for dyeing of polyester fabric was reported in the supporting information (Section **S2**) (Fig. 2).

2.5.2 Measurement for the Dyeing Properties

2.5.2.1 Fastness Properties According to the ISO 105-C02 (1989), ISO 105-X12 (1987), ISO 105-EO4 (1989), ISO 105-F04, and AATCC 16–2004 test methods, respectively, the colored PET fabrics fastness properties against washing, rubbing, perspiration, sublimation, and light were assessed [19].

2.5.2.2 Colorimetric Analysis The color parameters of the dyed PET fabric were measured using a spectrophotometer (Gretag Macbeth, CE 7000 A). The following CIELAB coordinates were measured: lightness (L^*), chroma (C^*), the degree of redness (+ve) and greenness (-ve) (a^*), and the degree of yellowness (+ve) and blueness (-ve) (b^*). The color strength (*K/S*) values were obtained according to the Kubelka–Munk equation (AATCC, 1991) [52].

2.5.2.3 Ultraviolet Protective Factor (UPF), UV-A and UV-B Transmission The *UPF* and ultraviolet radiation (UV-R) transmission through dyed was determined according to S/NZS 4399:1996 standard procedure. The ultraviolet transmission through the fabric was determined by a Cary Varian 300 UV–Vis spectrophotometer under AATCC 183:2010 UVA Transmittance [53–55]. The ability of textile fabrics to protect human skin from ultraviolet radiation is measured by the *UPF* (ultraviolet protection factor). The ratio of how long it takes for skin to become red (erythematous) when exposed to sunlight continuously is used to express it [56]. The following Eq. (1) is used to compute the *UPF* [57, 58]:

$$\mathrm{UPF} = \frac{\mathrm{MED}_{\text{protected skin}}}{\mathrm{MED}_{\text{unprotected skin}}} \tag{1}$$

where after 22 ± 2 h of continuous exposure, the minimum erythemal dose (*MED*) is the amount of radiant energy required to cause the first detectable reddening of skin. In Table 1, the various *UPF* ratings are listed.

2.6 Biological Section

2.6.1 Antimicrobial Evaluation

The bacterial strains used to evaluate the antibacterial activity of the dyes were two gram positive bacteria (*Staphylococcus aureus, Bacillus subtilis*), and two Gram-negative bacteria (*Escherichia coli, Pseudomonas aeuroginosa*). The anti-fungal activities of the compounds were tested against two fungi (*Candida albicans, Aspergillus flavus*) according to the method reported [59, 60] (Section **S3**). The *%ActivityIndex* for the complex was calculated by Eq. (2).

$$\%\ \text{Activity Index} = \frac{\text{Zone of inhibition by test compound (diameter)}}{\text{Zone of inhibition by standard (diameter)}} \times 100 \tag{2}$$

Table 1 Classification scheme for *UPF* rating

UPF rating	% UVR transmitted	Protection category
15–24	6.7–4.2	Good
25–39	4.1–2.6	Very good
40–50 +	≤ 2.5	Excellent

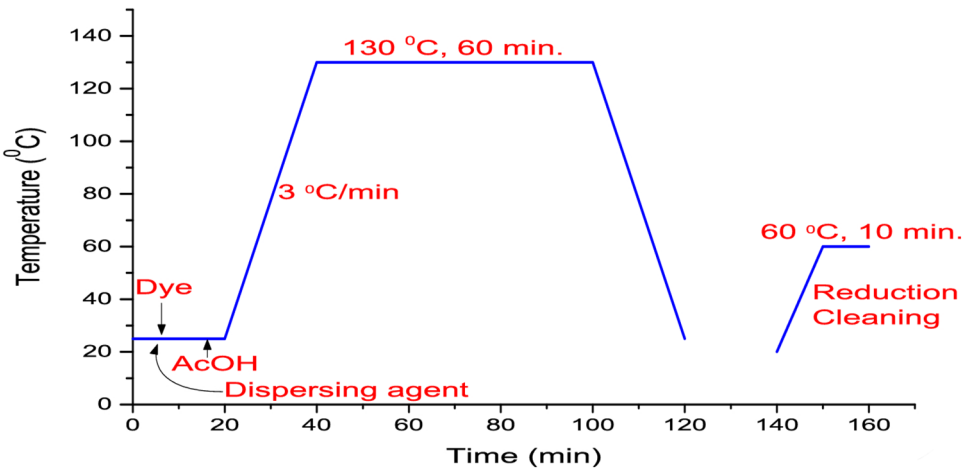

Fig. 2 Dyeing procedure of PET using the synthesized compounds

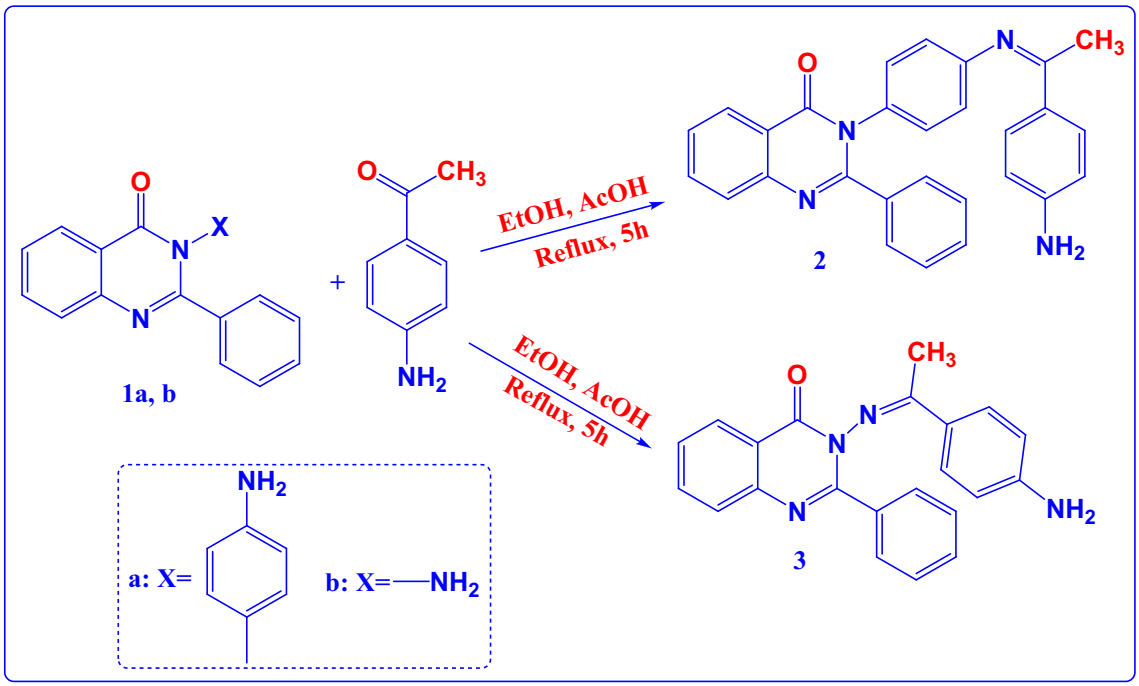

Scheme 1 Synthesis of compounds **2, 3**

3 Results and Discussion

3.1 Synthesis and Characterization

The starting compound **1a** and/or **1b** was condensed with *p*-amino acetophenone by one-pot two-component systems in the presence of ethanol and acetic acid to yield the corresponding compounds **2, 3** as shown in Scheme 1. The characteristic spectral analysis of FT-IR, ^{1}H-NMR, ^{13}C-NMR, and mass spectra used to verify the synthetic compounds' structural integrity are included in the supplementary file (Figs. S1–S4). The nucleophilic attack of the amine group on the electrophilic carbonyl carbon of the acetophenone to generate an imine is the first reversible step in the mechanism of azomethine synthesis. The formation of azomethine from an imine depends largely on the water removal rate in the final step. Depictions of compounds **2, 3** were established based on their elemental analyses and spectral data (FT-IR, ^{1}H-NMR, ^{13}C-NMR, and MS). The FT-IR absorption bands of the compounds **2, 3** appeared at 1600–1673 cm^{-1} for the C = N quinazolinone ring, and 1510–1517 cm^{-1} are due to azomethine group C = N– and the 1440–1510 cm^{-1} are due to the C = O of quinazolinone ring, respectively. The ^{1}H-NMR spectra revealed doublet signals at range δ 12.15–12.21 ppm can be attributed to the NH_2 protons which was exchangeable with D_2O, the singlet signal at 2.25–2.34 ppm is due to CH_3 protons. ^{13}C-NMR spectra of compounds **2**, **3** showed signals at δ 26.32–29.31 that belong to the (CH_3), signals at δ 170.54–170.58 ppm correspond to the (C = N imine), the signals at δ 165.23 ppm are due to (C = O quinazolinone), the signals at δ 154.03–159.52 ppm are attributed to the (C = N quinazolinone). The number of signals found is corresponding to the magnetically nonequivalent carbon atoms. Moreover, the mass spectra of the azomethine compounds **2, 3** displayed peaks at m/z which match their exact molecular mass. Details of selected spectroscopic data are reported in the experimental section.

The synthesis procedure for azo disperse dyes **4a–e and 5a-e** is shown in Schemes 2 and 3. The diazonium salts of compound 2, 3 coupling with different pyrazolone derivatives in pyridine yielded the corresponding compound **4a–e and 5a-e** in good yield. The structures of dyes **4a–e and 5a-e** were confirmed by means of FT-IR, ^{1}H-NMR, ^{13}C-NMR, mass spectrometry, and elemental analyses. Thus, the FT-IR spectra of dyes **4a–e and 5a-e** showed characteristic bands at 3349–3416 cm^{-1} and 1498–1587 cm^{-1} due to the N–H stretching vibration and the azo group (N = N) bending vibration, respectively. Moreover, a strong band at 1704–1727 cm^{-1} corresponding to the C = O group of the pyrazolone moiety and an absorption band at 1588–1987 cm^{-1} due to the C = N stretching vibration of the quinazolinone moiety were observed. The ^{1}H-NMR spectra of dyes **4a–e and 5a-e** exhibited a singlet signal ascribable to an NH proton at δ 12.05–12.23 ppm, which was exchangeable with D_2O for compound **4b** and **5b**, and a broad peak at δ 9.23–13.54 ppm, which can be attributed to enolic OH

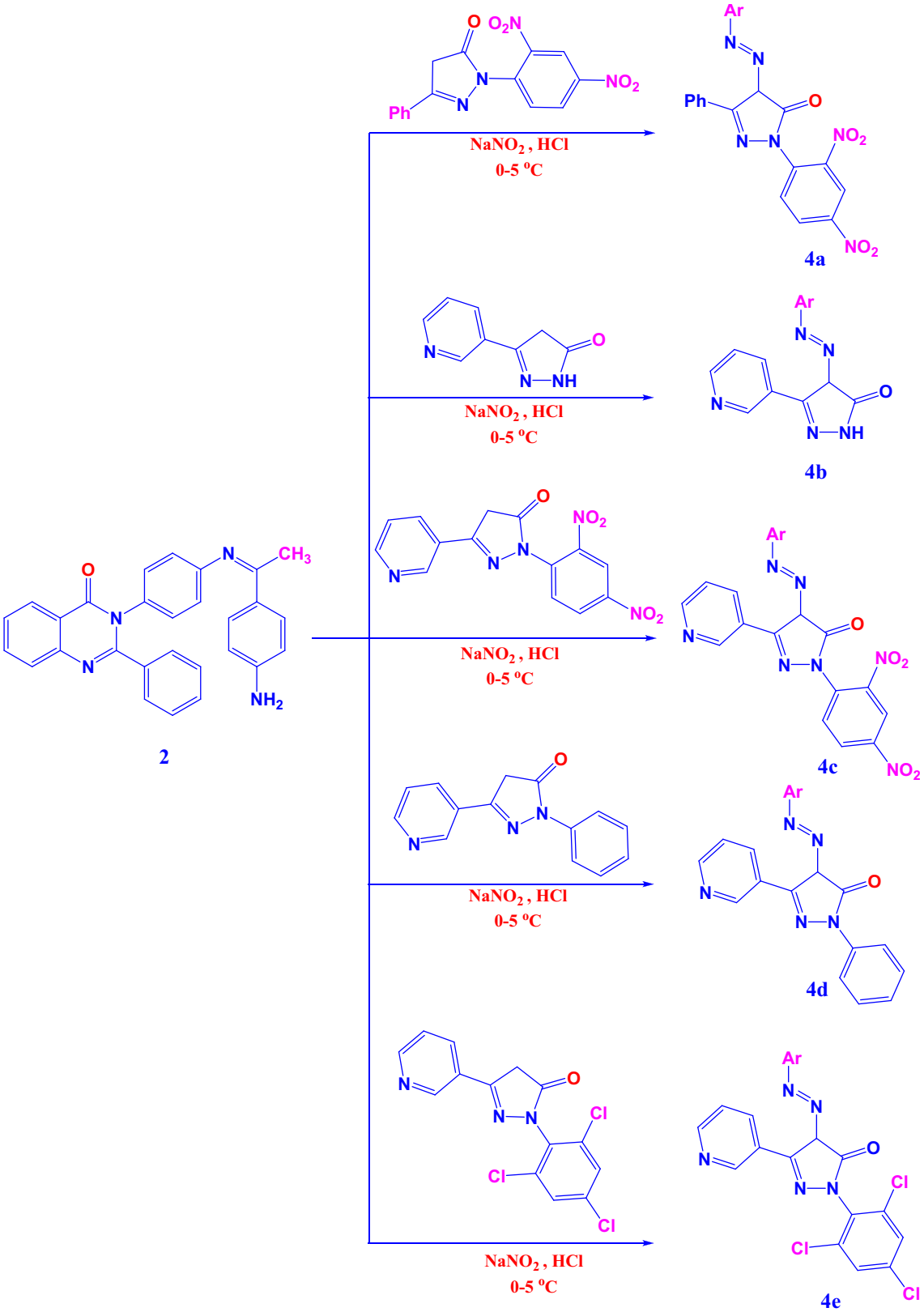

Scheme 2 Synthesis of compounds **4a-e**

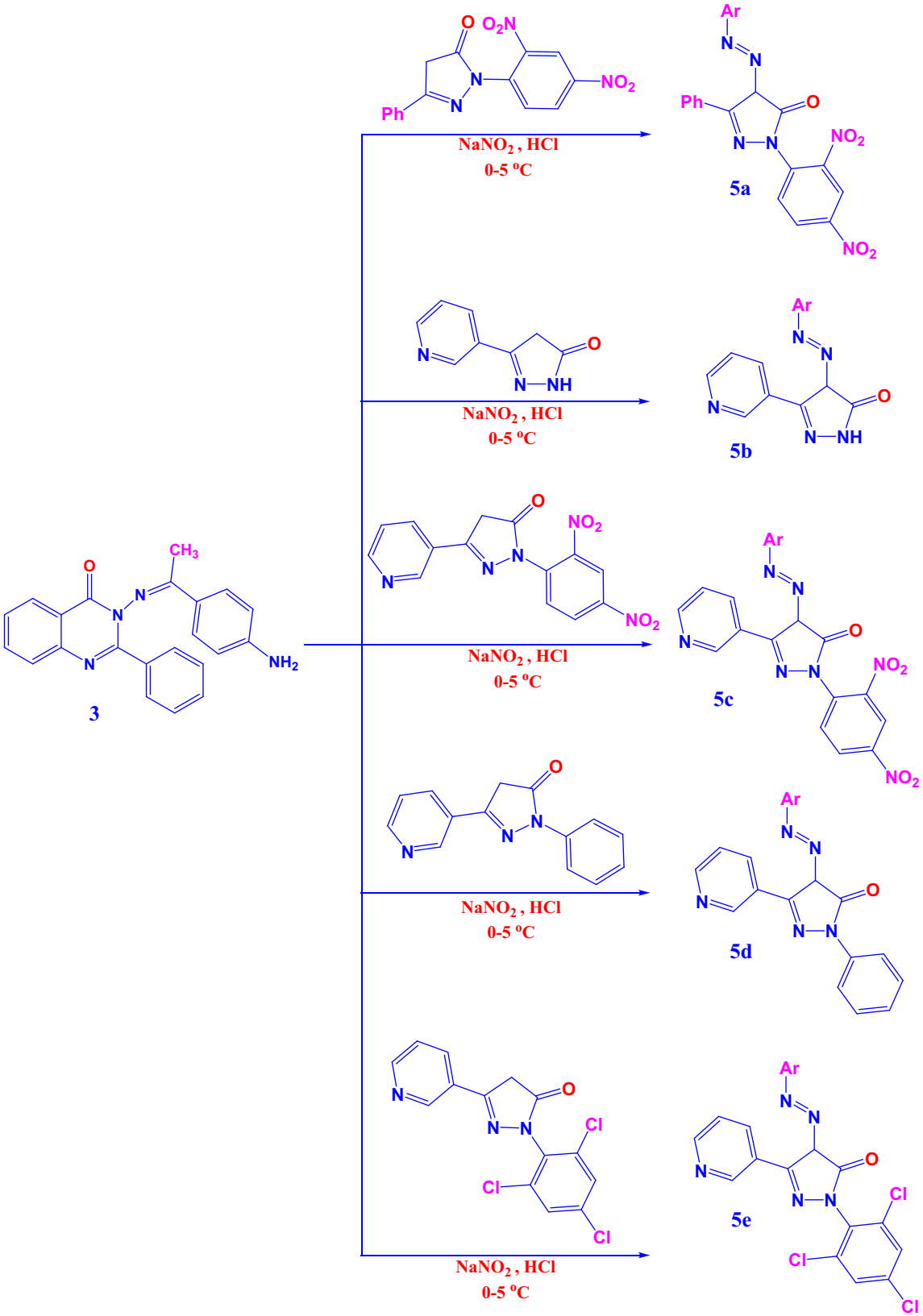

Scheme 3 Synthesis of compounds **5a-e**

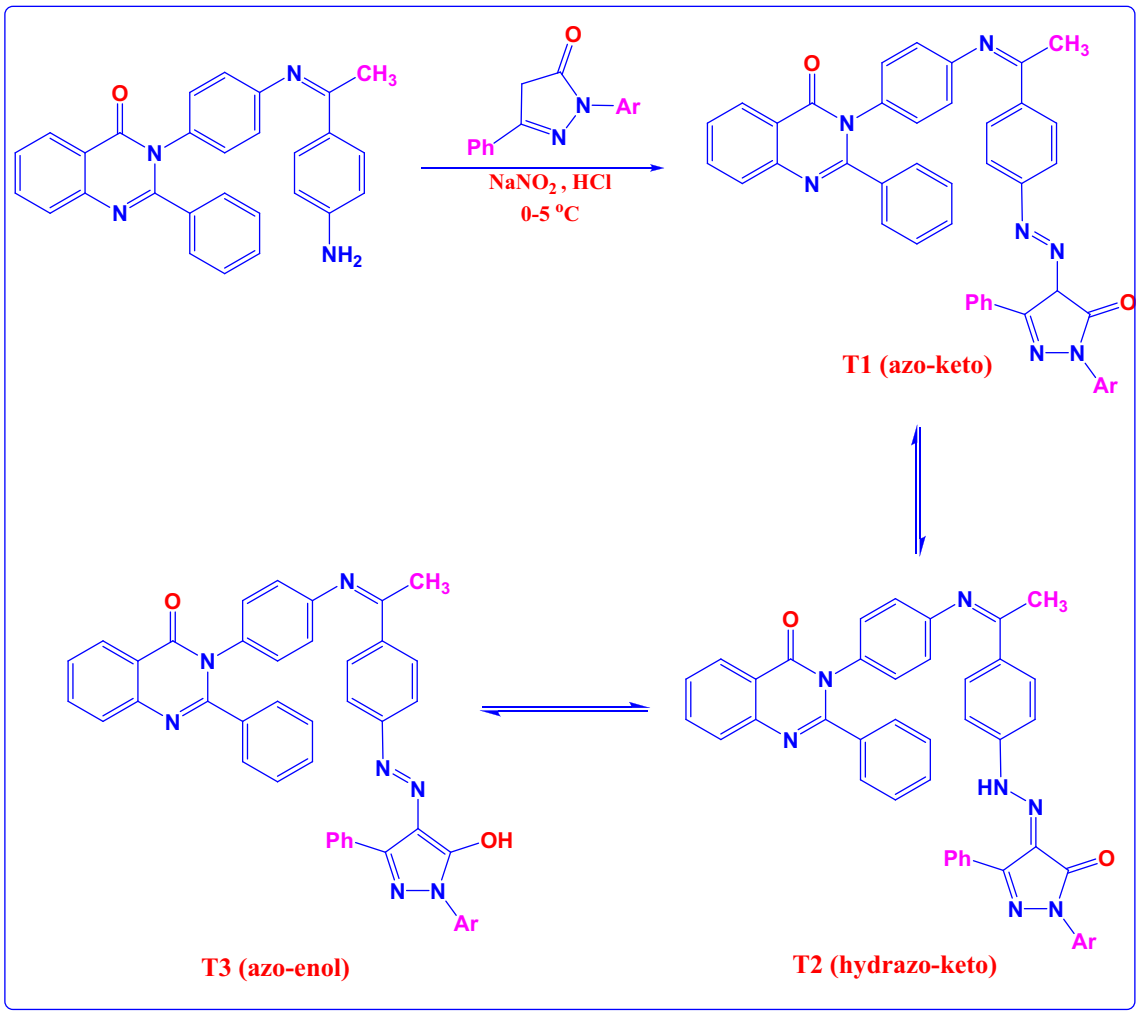

Scheme 4 Keto-enol tautomerism

or tautomeric hydrazone NH protons (keto–hydrazo or enol–azo forms). These results revealed that the single tautomeric form of the dyes is predominant in the solution state (**T2** or **T3** in Scheme 4), whereas the azo–keto tautomers are preferred in the solid state (Scheme 1). The ^{13}C-NMR spectral data of dyes **4a–e and 5a-e** were in accord with the predicted structures, and the mass spectra confirmed the expected molecular weights (see experimental section).

3.2 Visible Absorption Spectroscopic Properties of Dyes 4a–e and 5a-e

In general, heterocyclic-based azo disperse dyes have a stronger bathochromic effect than their benzenoid analogues, with larger solvatochromic effects because of their higher polarity, particularly in the excited state [61, 62]. In ethanol (a polar protic solvent), DMF (a dipolar aprotic solvent), and benzene (a nonpolar solvent), the electronic absorption spectra of the dyes **4a-e** and **5a-e** were measured at room temperature and quantified at a concentration of 10^{-5} mol/L. Results of λ_{max} and molar absorptivity (ε) are summarized in Table 2 and Figs. 3, 4, 5, 6, 7 and 8. Due to the

presence of electronic transitions in the conjugate system made up of phenyl rings, heterocyclic moieties, and the azo group, which can be classified as the π–π* transition type, all dyes displayed only one absorption maximum in the visible region in the range of 359–490 nm. Overall, it was discovered that the dye absorption maxima were influenced by the substituents' nature on N1 of pyrazolone moieties, position, as well as the diazo component.

3.2.1 Solvent Effect on the Absorption Spectra

Table 2 demonstrates that the dyes **4a-e** and **5a-e** were more sensitive to polar aprotic solvents than polar protic solvents or nonpolar solvents. The decreased contribution of ethanol to the transition energy as a polar protic solvent may be explained by the strong hydrogen bonding between the

Table 2 Absorption spectra of dyes **4a-e** and **5a-e**

No	Absorption λ_{max} (nm) (Benzene)	ε	Absorption λ_{max} (nm) (EtOH)	ε	Absorption λ_{max} (nm) (DMF)	ε
4a	411	1780	423	2000	490	2410
4b	373	965	388	1080	465	4109
4c	387	872	420	1240	483	1733
4d	376	755	405	1380	467	1156
4e	376	480	413	1220	477	2343
5a	407	1720	431	1120	435	2783
5b	359	670	389	1720	386	1100
5c	371	630	418	1780	430	1133
5d	360	778	396	1256	415	1099
5e	362	798	408	1324	421	1120

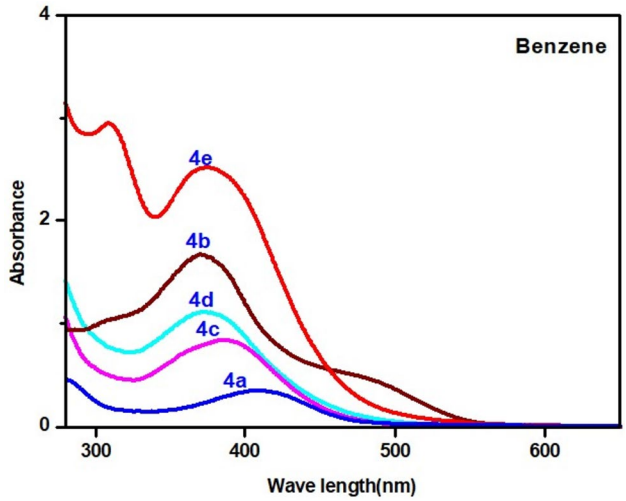

Fig. 3 Absorption spectra of dyes **4a-e** in benzene (3×10^{-5} M)

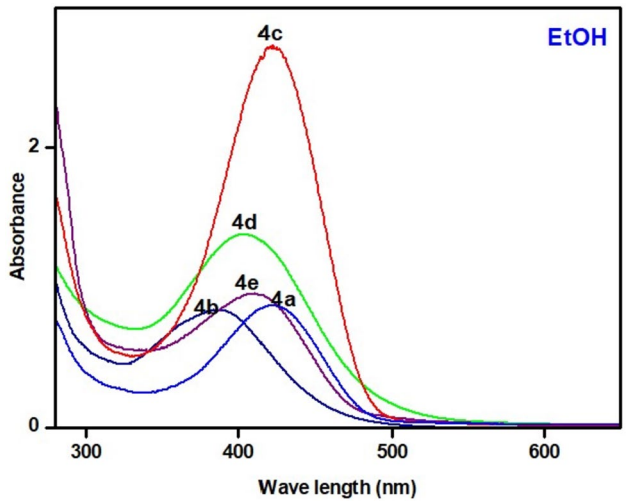

Fig. 5 Absorption spectra of dyes **4a-e** in EtOH (3×10^{-5} M)

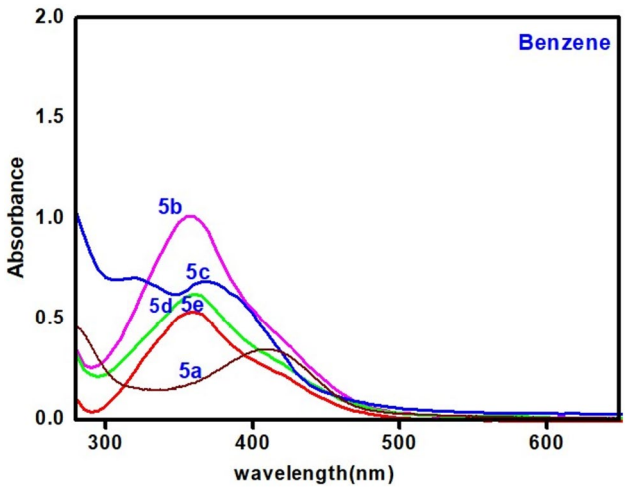

Fig. 4 Absorption spectra of dyes **5a-e** in benzene (3×10^{-5} M)

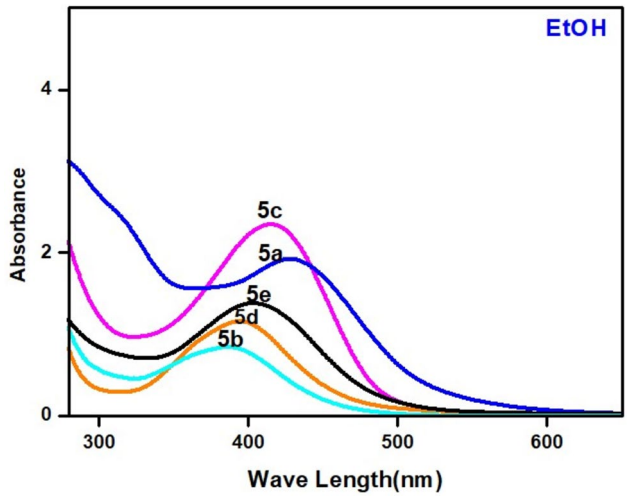

Fig. 6 Absorption spectra of dyes **5a-e** in EtOH (3×10^{-5} M)

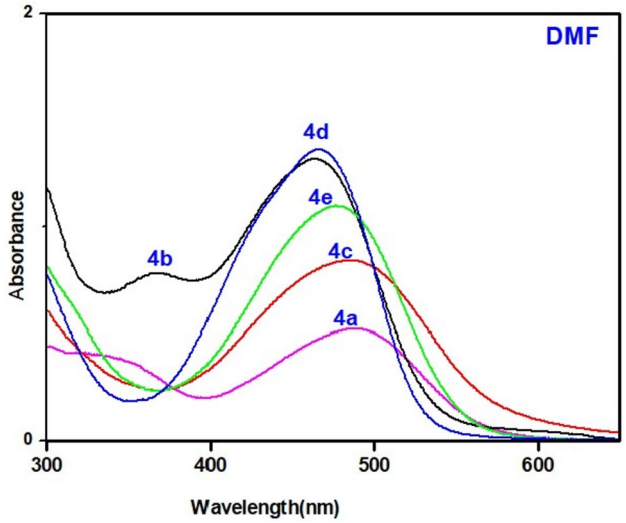

Fig. 7 Absorption spectra of dyes **4a-e** in DMF (3×10^{-5} M)

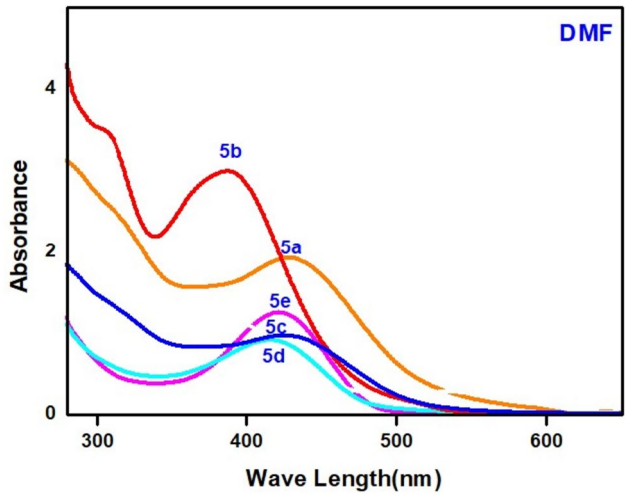

Fig. 8 Absorption spectra of dyes **5a-e** in DMF (3×10^{-5} M)

ethanolic hydrogen, nitrogen and oxygen centers. Due to DMF's polar and alkaline properties, which account for the majority of solute–solvent interactions, all dyes showed the maximum sensitivity in this solvent.

3.2.2 Substituent Effects on the Absorption Spectra

Because dyes **4a-e and 5a-e** contain π electrons, they can be subjected to UV–vis absorption measurements to determine the electron shell state. The main difference between dyes is the nature of the substituents on the pyrazolone moiety, i.e., di-NO_2 in **4a, 4c, 5a and 5c**, 3-Cl in **4e and 5e**, and phenyl in **4d**, and **5d**. As shown in Figs. 3, 4, 5, 6, 7 and 8, the order of λ_{max} was **4a > 4c > 4e > 4d > 4e, 5a > 5c > 5e > 5d > 5e,** respectively. The λ_{max} of dye **4a, 4c** (374–422 nm) and **4e** was higher than that of dye **4b** and **4d**, which is due to the bathochromic shift of the absorption band caused by the presence of the electron-withdrawing NO_2 and Cl group, respectively. In addition, the λ_{max} of dye **5a, 5c** and **5e** was higher than that of dye **5b** and **4d** (370–416 nm), which is due to the bathochromic shift of the absorption band caused by the presence of the electron-withdrawing NO_2 and Cl group, respectively. Additionally, the λ_{max} of a series of dyes **4a-e** higher than that of a series of dyes **5a-e** due to the bathochromic shift of the absorption band caused by the presence of the electron-withdrawing phenyl moiety. This result revealed that as the conjugation in the dye molecules increases or decreases, the absorption bands exhibit bathochromic or hypsochromic shifts, respectively. The extent of this shift depends most likely on the impact of the structural changes in the phenyl nucleus.

3.3 Dyeing Properties on Polyester Fabrics

3.3.1 Assessment of the Fastness Property

To assess the dyes' fastness qualities, 2% owf of the dyes were applied to polyester fabrics. The strong dye–dye and dye–fiber interaction energy, which prevents the dye molecule from moving to the fiber surface, is responsible for the very good washing fastness values of (**4**), as shown in Table 3, 4. Furthermore, a remarkable color levelling was obtained after washing, revealing the excellent penetration and affinity of the dyes for the fabric, and the dyes' inclusion

Table 3 Shade of fabric samples dyed with **4a-e and 5a-e** at 2% of level

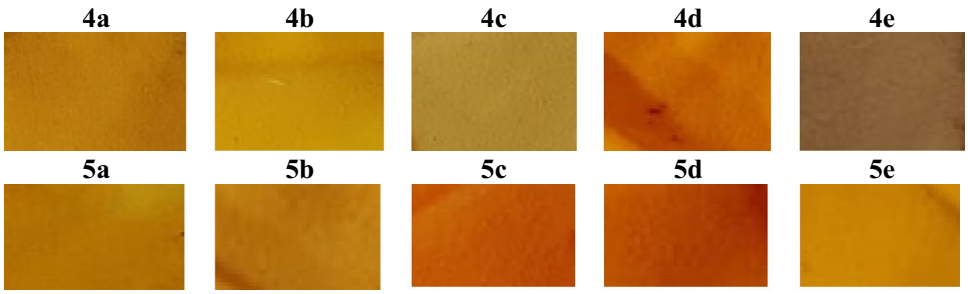

Table 4 Evaluation of fastness properties of synthesized dyed on polyester

Dyes No	Washing fastness			Rubbing fastness		Perspiration fastness						Sublimation		Light fastness
						Acidic			Alkaline					
	Alt	St.*	St.**	Dry	Wet	Alt	St.*	St.**	Alt	St.*	St.**	210	180	
4a	4	4	4	4–5	4	4	4	4	4	4	4	3–4	4	4
4b	4	4	4	4–5	4	4	4	4	4	4	4	3–4	4	4
4c	4	4	4	4–5	4	4	4	4	4	4	4	4	4–5	4–5
4d	4	4	4	4–5	4	4	4	4	4	4	4	3–4	4	4
4e	4	4	4	4–5	4	4	4	4	4	4	4	3–4	4	4
5a	4	4	4	4–5	4	4	4	4	4	4	4	3	34	4
5b	4	4	4	4–5	4	4	4	4	4	4	4	3	3–4	4
5c	4	4	4	4–5	4	4	4	4	4	4	4	4	4–5	4
5d	4	4	4	4–5	4	4	4	4	4	4	4	4–5	4–5	4–5
5e	4	4	4	4–5	4	4	4	4	4	4	4	3–4	− 4	4

St.* Staining on cotton, St. ** Staining on wool, Alt. Alteration in color

Rate for light fastness: 4–8 (acceptable), 1–3 (not acceptable); rate for different fastness:3–5 (acceptable), 1–2 (not acceptable)

of a hydrophobic group (C = O) prevents them from migrating back to the washing solution bath. Fastness to both acidic and alkaline perspiration was very good (**4**). These findings show that the dyes are stable in both alkaline and acidic media. Because of the high rate of dye molecule absorption into the materials, the rubbing fastness (both wet and dry) had excellent values (**4–5**). All of the synthesized dyes have good to very good sublimation fastness properties, which helped to produce a high molecular absorption coefficient as opposed to merely large dye movement at high temperatures. All of the synthesized dyes had very good light fastness (**4, 4–5**) fastness properties. The good fastness properties may be attributed to the strong dye–dye interaction energy that can prevent dye molecules from migrating to the fiber surface and the covalent bonding between the dye and the fiber. Due to the dyes' excellent substance compatibility with the fiber, all showed strong color yields.

3.3.2 Color Assessment

After application to polyester fabrics, dyes **4a–e and 5a-e** showed good color depth and leveling qualities owing to the presence of chromophores in their structures (Table 5). According to the color coordinates, polyester fabrics with good evenness, brightness, and color depth had a good affinity for the dyes. The darkness or lightness of the dyes on polyester fabrics was measured by comparing the L^* values, where positive and negative values correspond to lightness and darkness, respectively. As shown in Table 4, the L^* values of dyes **4a–e and 5a-e** vary from (59.99–74.84). Dyes **5, 10** and **11** are lighter compared with the other dyes. All the dyes are shifted to the reddish direction on the red-green axis according to the positive values of a^*. Also, all the dyes are shifted to the yellowish direction on the yellow-blue axis according to the positive values of b^*. These results demonstrate that the investigated dyes had good affinity as well as good leveling properties according to the visual observations of the colored fabrics.

Table 5 Optical measurements of all synthesized dyes on polyester fabrics (light source D65/10° observer)

Dyes no	L^*	a^*	b^*	ΔE
4a	63.85	8.34	52.16	66.36
4b	71.91	6.8	63.31	75.42
4c	68.97	5.43	46.38	59.24
4d	59.99	25.81	69.98	87.09
4e	64.87	3.69	26.19	24.23
5a	64.60	7.62	62.74	75.81
5b	71.57	5.41	58.73	70.59
5c	74.84	2.71	33.56	45.41
5d	60.43	24.41	67.08	83.91
5e	67.31	12.53	67.08	80.1

3.3.3 Effect of pH on the Color Strength

One of the most important factors to consider when determining the best dyeing conditions for a dispersion dye on polyester fabrics is the pH of the dye bath. A series of dyeing tests were conducted using a dye concentration of 1% owf and a series of dyeings were carried out by varying the dyebath pH from 3 to 11 at a dyeing temperature of 130 °C to examine the color strength of dyed polyester in terms of *K/S* on polyester fabrics. As shown in (Fig. 9 and Table 6). Dyes **4d, 5a-d** dyes give higher *K/S* values at pH **3** while dyes **4b, 4e and 5e** give highest color strength (*K/S*) values at pH **5** and a better color yield on polyester fabrics was obtained

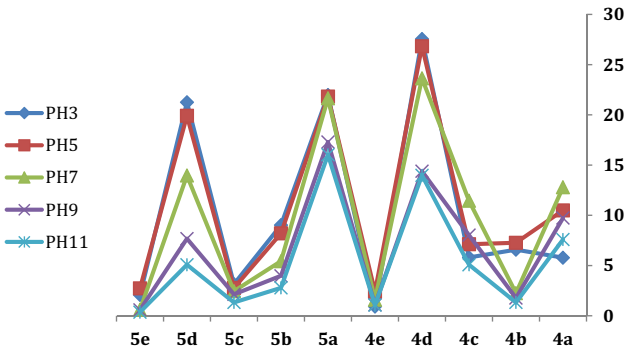

Fig. 9 Effect of dyeing pH on (*K/S*) values of polyester fabric dyed

Table 6 Effect of dyeing pH on the color strength (*K/S*) values of polyester fabric dyed with dyes **4a-e** and **5a-e**

Dye no	*K/S*				
	PH3	PH5	PH7	PH9	PH11
4a	5.78	10.49	12.80	9.73	7.59
4b	6.58	7.27	2.25	1.78	1.33
4c	5.81	7.12	11.45	8.03	5.08
4d	27.55	26.83	23.64	14.39	13.98
4e	0.92	2.39	1.59	1.09	1.07
5a	21.98	21.82	21.65	17.30	16.03
5b	9.02	8.20	5.43	3.98	2.78
5c	3.15	2.77	2.45	2.13	1.33
5d	21.25	19.91	13.96	7.68	5.08
5e	2.07	2.73	0.60	0.59	0.36

at higher pH **7** for dye **4a, 4c**. Moreover, in the most cases of dyes a more pronounced decrease in the dye uptake with increasing the pH (**9, 11**) was observed compared with dyes **4d**, and **5a**, which may be attributed to the higher aggregation of dyes due to its higher molecular weight.

3.3.4 Effect of the Dyeing Time on the Color Strength

The influence of dyeing time on the exhaustion percentage for dyes **4a–e and 5a-e** was determined using a dye concentration of 2% owf at pH 8 on polyester fabrics (Fig. 10 and Table 7). The results revealed that the amount of dye adsorbed on fabrics increased with an increase in the dyeing time. The percentage of dye exhaustion increased significantly in the early stages of dyeing (until 60 min) probably due to its high substantivity and then increased gradually in the last 60 min until reaching equilibrium at 110 min of dyeing time for fabrics. It was also found that the total fixation yield of the dyes increased as the dyeing process progressed, i.e., higher color strength values were observed.

3.3.5 Effect of Dye Concentration on Color Strength

Relationship of *K/S* value at the maximum wavelength and dye amount was established for synthesized 4**a-d** and **5a-e** and shown in (Fig. 11 and Table 8). If there is enough dye present to saturate the fiber at high dye concentrations, the depth of shadow generally increases as the availability of the dye molecules in the dye bath also increases, allowing for more dye molecules to attach to the fiber. Additionally, high dye concentration results in more accessible dye sites on the fiber and less competitive hydrolysis, which raises the *K/S* value. The results show that the *K/S* value of dyed fabric increased gradually as the dye concentration shifted from 1 to 3%. Therefore, a dye concentration of 3% owf was determined to afford the optimum exhaustion.

3.3.6 Ultraviolet Protection Factor (UPF)

Since covering up with clothing is the most practical and natural approach to shield the body from the elements, there is a growing demand on the market for apparel that can provide effective UV radiation protection. The link between sun

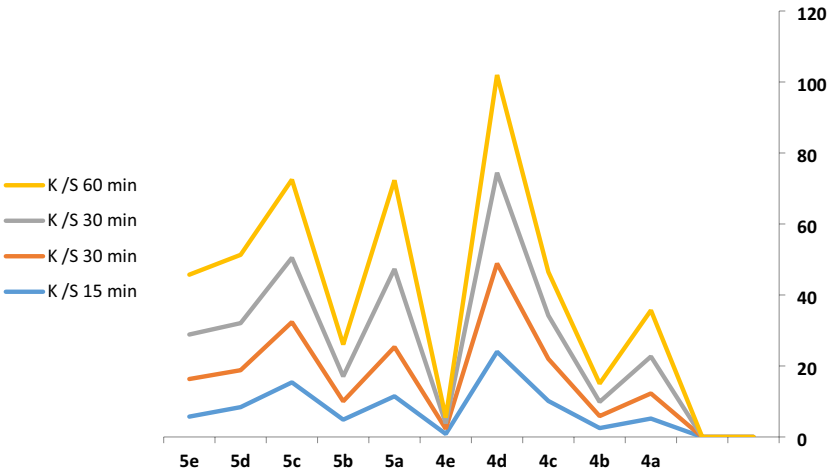

Fig. 10 Effect of dyeing time on (*K/S*) values of polyester fabric dyed

Table 7 Effect of dyeing time on the color strength (*K/S*) values of polyester fabric dyed with synthesized dyes

Dye no	*K/S*			
	15 min	30 min	45 min	60 min
4	5.18	7.08	10.4	13.01
5	2.5	3.38	4	5.16
6	10.14	11.86	12.22	12.27
7	24	24.86	25.58	27.53
8	0.84	1.45	1.52	1.65
9	11.46	13.88	21.97	25
10	4.87	5.18	7.01	8.98
11	15.38	16.98	18.12	22.01
12	8.4	10.41	13.26	19.24
13	5.73	10.59	12.54	16.86

exposure and various forms of skin cancer, accelerated skin ageing, cataracts, and other eye conditions is widely known. There is evidence that UV light reduces the effectiveness of the immune system. Blocking of UV is dependent on multiple factors, including fiber type, synthesis of dyes, fabric construction and dyeing, as a darker color increases protection [63]. Because of the "hole effect," UV textiles are typically made entirely of synthetic fibers such as polyester and nanofibers that are woven tightly together to allow for much less direct skin exposure to UVR [64]. Excellent *UPF* ratings were obtained by polyester fabrics, far exceeding a *UPF* of 50. Low fabric porosity has been linked to the polyester clothing's success in lowering UVR transmittance, suggesting that clothing with higher BSA coverage can serve as a stronger barrier against sun exposure and lessen the need for sunscreen application [64].

Tables 9 provide the polyester fabric's UV protection factor results for all synthetic dyes. The *UPF* rating for **4a-e** dyed polyester is excellent, with a value in the range of **25.49–152.23** except dye **4a** is very good *UPF*. This means that the transmittance percentage in the UV-B region of 290–315 nm is 0.01–0.06, and the UV-A range of 315–400 nm is 0.01–0.09, respectively, (blocking 100%) of the UV light.

For **5a-e** dyed polyester the *UPF* rating is excellent, with a value in the range of **38.60–177.32** except dye **5d** is very good *UPF*. This means that the transmittance percentage in the UV-B region of 290–315 nm is 0.01–0.06, and the UV-A range of 315–400 nm is 0.01–0.09, respectively, (blocking 100%) of the UV light. As a result, all synthesized dyes provide the textile material with excellent ultraviolet Protection (Fig. 12 and Table 9). Based on the previous results [65], protection from ultraviolet radiation increases with the increase brighter-colored fabric dyes, and since all the synthesized dyes are distinguished by the brightness of the color, Blocking of UV of these dyes are excellent. Furthermore, the reason that *UPF* values are higher on polyester

Table 8 Effect of dye concentration on the color strength (*K/S*) values of polyester fabric dyed with synthesized dyes

Dye no	*K/S*			
	0.5%	1%	2%	3%
4a	2.01	2.37	3.12	3.89
4b	2.48	4.8	7.56	8.47
4c	1.72	2.81	2.97	4.7
4d	8.68	9.74	12.02	18.19
4e	0.94	1.25	1.45	3.18
5a	3.14	13.01	14.63	25.67
5b	4.02	15.32	17.12	18.97
5c	2.00	4.2	11.33	12.2
5d	18.09	20.73	21,06	26.63
5e	2.23	6.23	11.78	16.11

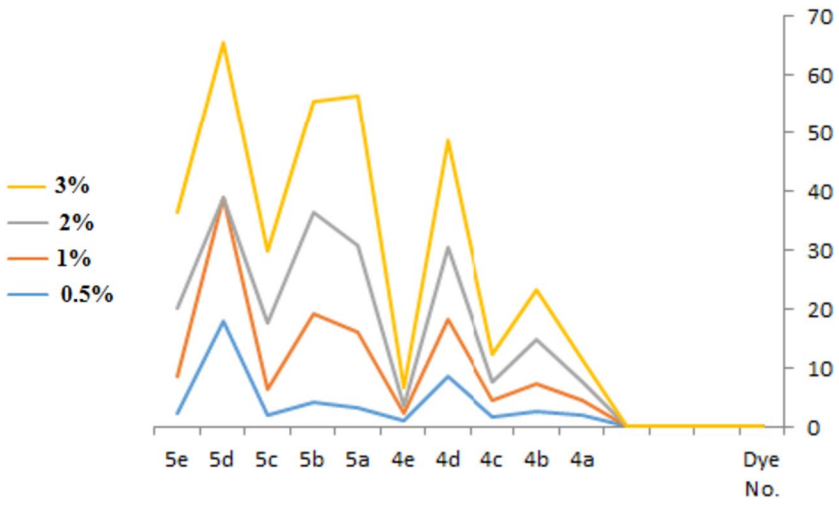

Fig. 11 Effect of dye concentration on (*K/S*) values of polyester fabric dyed

Table 9 Ultraviolet protection factor rating

Dyes no	*UPF* range	Protection category	Effective UV-R transmission (%)	
			UV-B[a]	UV-A[b]
4a	25.49	Very good	0.06	0.09
4b	60.63	Excellent	0.03	0.03
4c	152.23	Excellent	0.01	0.01
4d	65.51	Excellent	0.02	0.01
4e	57.76	Excellent	0.03	0.02
5a	45.04	Excellent	0.04	0.05
5b	107.42	Excellent	0.01	0.01
5c	56.11	Excellent	0.04	0.03
5d	38.60	Very good	0.07	0.06
5e	177.32	Excellent	0.01	0.01

UV-B[a] Transmittance (mean transmittance percentage in the range (290–315 nm)

UV-A[b] Transmittance (mean transmittance percentage in the range (315–400 nm)

fabric may be explained by the larger percentage of dye exhaustion and compact structure of polyester fabric.

3.4 Antibacterial Activity

Gram-positive and Gram-negative pathogen bacteria are responsible for an alarming rise in infectious diseases that are fatal [66]. The antibiotic is currently one of the most effective tools against infectious diseases. However, the development of antibiotic resistance and the scarcity of recently created antimicrobial drugs represent a serious threat to human and animal health [67]. One of the most effective approaches to lower antimicrobial resistance is the prudent use of antibiotics. One of the most active areas of study to reduce the risk of contagious diseases brought on by hazardous bacteria, fungi, viruses, and parasites is the quest for compounds with highly antimicrobial action [68]. This severe effect causes researchers to synthesize more effective antibacterial agents. The heterocyclic dyes containing quinazolinone have received great attention in biological and pharmacological fields due to their significant broad antimicrobial spectrum [69–71]. This has a strong impact, leading our group to synthesize antibacterial agents more effectively. The synthesized dyes **4a-e** and **5a-e** were tested for their in vitro antibacterial activities against a panel of two gram positive bacteria (*S. aureus*, *B. subtilis*), and two-Gram negative bacteria (*E. coli*, *P. aeuroginosa*). The anti-fungal activities of the compounds were tested against two fungi (*C. albicans*, *A. flavus*). The diameter of inhibition zones (IZ) of the newly synthesized compounds were compared with the reference drugs Ampicillin and Clotrimazole. The obtained results are presented in (Table 10, Fig. 13), in general, for Gram-negative bacteria (E. coli) dyes **4a, 5a, and 5e** displayed very good activities, dyes **5c and 5d** displayed moderate activities, dyes **4b** and **4c** displayed weak activities, while dyes **4d** and **5b** gave no activities comparison with reference drug ampicillin. For *P. aeuroginosa* strains dyes **4a, 5a, 5c, 5d and 5e** displayed very good activities, dyes **4b**, **4c** and 4e displayed weak activities, while dyes **4d** gave no activities in comparison with reference drug ampicillin. For Gram-positive bacteria (*S. aureus*) dyes **4a, 4e, 5c, 5d and 5e** displayed very good activities, dyes **4b, 4c, 4e and 5e** displayed moderate activities, while dye **4d** gave no activities in comparison with reference drug ampicillin. for Gram-negative bacteria (*B. subtilis*) dyes **4a, 5a, 5c, and 5e** displayed highest activities, dyes **4b, 4c, and 5d** displayed very good activities, dyes **4e** and **5b** displayed moderate activities, while dye **4d** gave no activities in

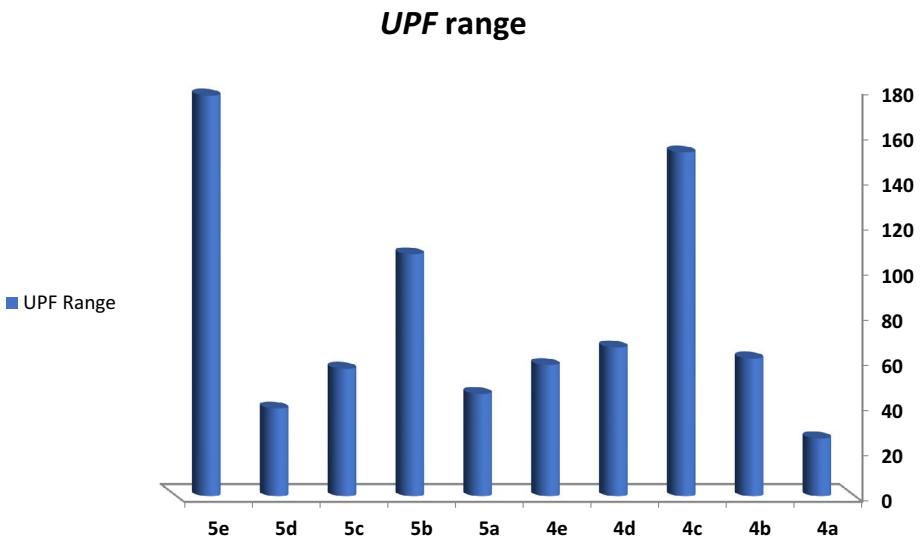

Fig. 12 Inhibition zones (mm) of novel compounds against different bacteria and fungi

Table 10 Diameters of inhibition zones (mm) of synthesized dyes **4a-e,** and **5a-e** against different tested bacteria and fungi at 37 °C after 24 h

Compound	*E. coli*		*P. aeurogino sa*		*S. aureus*		*B. subtilis*		*C. Albicans*		*A. flavus*	
	Diameter of inhibition zone (mm)	% Activity index	Diameter of inhibition zone (mm)	% Activity index	Diameter of inhibition zone (mm)	% Activity index	Diameter of inhibition zone (mm)	% Activity index	Diameter of inhibition zone (mm)	% Activity index	Diameter of inhibition zone (mm)	% Activity index
4a	11	44.0	14	60.9	12	50.0	16	69.6	19	70.4	18	72.0
4b	6	24.0	8	34.8	9	37.5	10	43.5	12	44.4	11	44.0
4c	5	20.0	6	26.1	7	29.2	10	43.5	11	40.7	10	40.0
4d	NA	–	NA	–	NA	–	NA	–	5	18.5	NA	–
4e	3	12.0	5	21.7	6	25.0	7	30.4	10	37.0	8	32.0
5a	12	48.0	16	69.6	12	50.0	17	73.9	21	77.8	19	76.0
5b	NA	–	3	13.0	6	25.0	8	34.8	9	33.3	6	24.0
5c	9	36.0	12	52.2	11	45.8	15	65.2	14	51.8	13	52.0
5d	9	36.0	11	47.8	10	41.7	13	56.5	16	59.2	14	56.0
5e	14	56.0	17	73.9	13	54.2	19	82.6	17	63.0	16	64.0
Ampicillin	25	100	23	100	24	100	23	100	NA	–	NA	–
Colitrimazole	NA	–	NA	–	NA	–	NA	–	27	100	25	100

comparison with reference drug ampicillin. With respect to antifungal activity, all dyes exhibited very good to excellent activities against *C.albicans*, while dyes **4d** and **5b** displayed moderate activities against *C. albicans* in comparison with the reference drug Colitrimazole. Moreover, dyes **4a, 5a, and 5e** displayed highest activities, dyes **4b, 4c, 5c, and 5d** displayed very good activities, dyes **4b** and **5b** displayed moderate activities, while dyes **4d** gave no activities against *A. flavus* in comparison with reference drug Colitrimazole. The above data demonstrated that the slight change in the molecular configuration of the tested compounds strongly affected antimicrobial activity.

4 Conclusion

In conclusion, disperse Quinazolinone dyes **4a–e and 5a-e** based on pyrazolone moieties were synthesized in good yields. Spectroscopic and elemental analyses were used to determine the structure of the synthesized dyes. The dyes were successfully applied to polyester fabrics to produce shades with satisfactory color evenness and color depth. Dyes **4a–d**e and **5a-e** showed good fastness to light (**4, 4–5**). Fastness to both acidic and alkaline perspiration was very good (**4**), the rubbing fastness (both wet and dry) had excellent values (**4–5**), and very good washing, sublimation fastness (**4**). According to the color coordinates, the dyes exhibited an excellent affinity for polyester fabrics with good to very good brightness and color depth. For dyeing polyester fabrics, the best pH and dyeing temperature was 5 and 130 °C, respectively. The percentage of dye exhaustion increased significantly in the early stages of dyeing (until 60 min) probably due to its high substantivity and then increased gradually in the last 60 min until reaching equilibrium at 110 min of dyeing time for fabrics. A dye concentration of 3% owf was determined to afford the optimum exhaustion. The *UPF* rating for dyed polyester is excellent; with a value in the range of 38.60–177.32 except dye **4a** is very good *UPF*. The results of color strength tests were excellent, which demonstrates that the dyes showed a high level of fabric attraction and solubility. Furthermore, their remarkable degree of evenness indicates their good diffusion, penetration, and fabric affinity. The newly synthesized dyes also exhibited antimicrobial properties, which render them promising as safe, disperse dyes for fabrics with antimicrobial effect. Considering that the synthesis of these dyes is simple and inexpensive and that they show dyeing qualities comparable to those of commercial dyes, this study provides access to a new group of dyes to satisfy the growing demand for dyes in the textile industry.

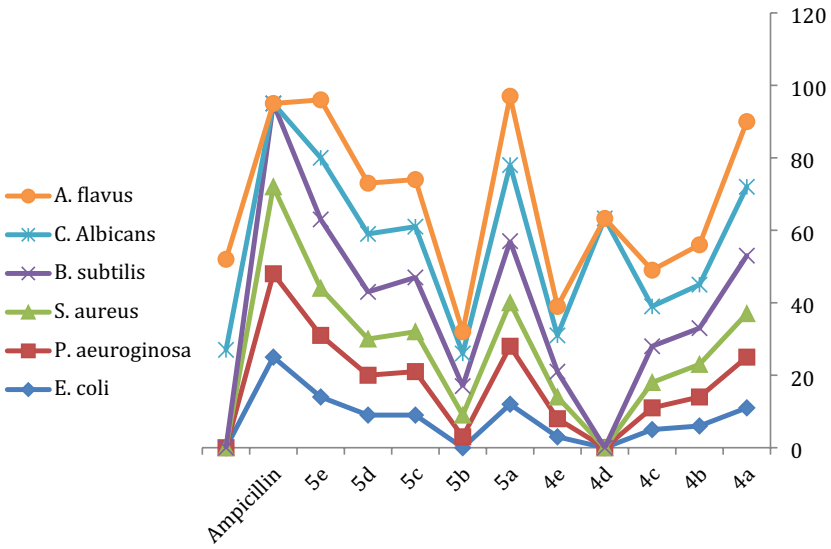

Fig. 13 *UPF* blocking (%) of dyed on polyester fabrics

Supplementary Information The online version contains supplementary material available at https://doi.org/10.1007/s12221-024-00507-6.

Funding Open access funding provided by The Science, Technology & Innovation Funding Authority (STDF) in cooperation with The Egyptian Knowledge Bank (EKB).

Data Availability The data that support the findings of this study are included within the article and supplementary file.

Declarations

Conflict of Interest The authors declare that they have no known competing financial interests or personal relationships that could have appeared to influence the work reported in this paper.

References

1. J. Oh, S.S. Kim, K.H. Kim, J. Lee, C. Kang, J. Supercrit. Fluid. **170**, 105 (2021)
2. S. Yu, H. Zhang, L. Pei, S. Liang, A. Dong, J. Wang, Fibers Polym. **23**, 443 (2022)
3. G.S. Shankarling, P.P. Deshmukh, A.R. Joglekar, J. Environ. Chem. Eng. **5**, 3302 (2017)
4. J.K. Adu, C.D. Amengor, N.M. Ibrahim, C. Amaning-Danquah, C.O. Ansah, D.D. Gbadago, J. Trop. Med. **2020**, 4850492 (2020)
5. G.A.M. Nawwar, K.S. Abdel Zaher, E. Shaban, N.M.A. El-Ebiary, Fibers Polym. **21**, 1293 (2020)
6. C. Gao, T. Xing, X. Hou, G. Chen, RSC Adv. **9**, 19791 (2019)
7. V.M. Dembitsky, T.A. Gloriozova, V.V. Poroikov, Nat. Prod. Bioprospect. **7**, 151 (2017)
8. M.A. Gouda, H.F. Eldien, M.M. Girges, M.A. Berghot, J. Saudi Chem. Soc. **20**, 151 (2016)
9. N.M. Mallikarjuna, J. Keshavayya, J. King Saud Univ. Sci. **32**, 251 (2020)
10. A. Gičević, L. Hindija, A. Karačić, In book: CMBEBIH 2019 (2020) https://www.springerprofessional.de/en/toxicity-of-azo-dyes-in-pharmaceutical-industry/16716466
11. R.M. Rohini, K. Devi, S. Devi, Der Pharm. Chem. **7**, 77 (2015)
12. M.N. Khan, D.K. Parmar, D. Das, Mini-Rev. Med. Chem. **21**, 1071 (2021)
13. A.M. Khedr, H. El-Ghamry, M.A. Kassem, F.A. Saad, N. El-Guesmi, Inorg. Chem. Commun. **108**, 107496 (2019)
14. M.A. Muhammad-Ali, H. Hamza Salman, E. Jasim, Asian J. Pharm. Clin. Res. **12**, 479 (2019)
15. S.S. Ragab, A.M. Sweed, K.Z. Hamza, E. Shaban, A.A. ElSayed, Fibers Polym. **23**, 2114 (2022)
16. K.M. Hassan, S. El-khabiry, G.M. ElHaddadd, A.B. Sallam, I. ElSayed, Curr. Chem. Lett. **11**, 83 (2022)
17. S. KofiKyei, O. Akaranta, Sci. Afr. **8**, e00406 (2020)
18. S. Benkhaya, S. M'Rabet, A. El Harfi, Inorg. Chem. Commun. **115**, 107891 (2020)
19. R.A. Abbas, A.E. Abd, A.J. Almonuim, S.K.T. Jarad, P. Constantin, Rev. Chim. **71**(6), 1 (2020)
20. F. Borbone, A. Carella, L. Ricciotti, A. Tuzi, A. Roviello, A. Barsella, Dyes Pigm. **88**, 290 (2011)
21. S. Irmuminova, B. Sezgin, T. Tilki, J. Sci. **15**(2), 319 (2020)
22. O.V. Kovalchukova, M.A. Ryabov, P.V. Dorovatovskii, Y.V. Zubavichus, A.N. Utenyshev, D.N. Kuznetsov, O.V. Volyansky, V.K. Voronkova, V.N. Khrustalev, Polyhedron **121**, 41 (2017)
23. F.M. Al-Mudhaffer, Y.A. Al-Ahmad, M.Q.A. Hassan, A.C. Emshary, Optik **127**, 1160 (2016)
24. A.M. El-badrawy, N. Nagy, E. Abdel-Latif, A.A. Fadda, Biointerface Res. Appl. Chem. **11**(5), 12937 (2021)
25. T. Aysha, M. El-Sedik, S. Abd El Megied, H. Ibrahim, Y. Youssef, R. Hrdina, Arab. J. Chem. **12**, 225 (2019)
26. H.K.A. Taha, H.J. Mohammed, JPTCP **30**(13), 193 (2023)
27. P. Bhawna, G. Bharghav, Nat. J. Pharm. Sci. **1**(1), 34 (2021)

28. S.A. Ibrahim, A. Ragab, H.A. El-Ghamry, Appl. Organomet. Chem. **36**, e6508 (2022)
29. Z. Zhao, X. Dai, C. Li, X. Wang, J. Tian, Y. Feng, J. Xie, C. Ma, Z. Nie, P. Fan, M. Qian, X. He, S. Wu, Y. Zhang, X. Zheng, Eur. J. Med. Chem. **186**, 111893 (2020)
30. W. Dohle, F.L. Jourdan, G. Menchon, A.E. Prota, P.A. Foster, P. Mannion, E. Hamel, M.P. Thomas, P.G. Kasprzyk, E. Ferrandis, M.O. Steinmetz, M.P. Leese, B.V.L. Potter, J. Med. Chem. **61**, 1031 (2018)
31. S. Wang, M. Gao, G. Tan, H. Ma, Y. Zhao, H. Du, Z. Wang, H. Chen, X. Li, Chin. J. Org. Chem. **37**, 385 (2017)
32. R. Bouley, D. Ding, Z. Peng, M. Bastian, E. Lastochkin, W. Song, M.A. Suckow, V.A. Schroeder, W.R. Wolter, S. Mobashery, M. Chang, J. Med. Chem. **59**, 5011 (2016)
33. B.N. Ravi, J. Keshavayya, V. Kumar, S. Kandgal, J. Mol. Struct. **1204**, 127493 (2020)
34. B. Manjunatha, Y.D. Bodke, J. Mol. Struct. **1244**, 130933 (2021)
35. R. Patel, K.C. Patel, Arab. J. Sci. Eng. **37**, 1347 (2012)
36. A. Demirçalı, F. Karcı, F. Sari, Color. Technol. **137**, 280 (2021)
37. A. Demirçalı, F. Karcı, O. Avinc, A.U. Kahrıman, G. Gedik, E. Bakan, J. Mol. Struct. **1181**, 8 (2019)
38. E.M. Rufchahi, H. Pouramir, M.R. Yazdanbakhsh, H. Yousefi, M. Bagheri, M. Rassa, Chin. Chem. Lett. **24**, 425 (2013)
39. S. Shinde, N. Sekar, Dyes Pigm. **168**, 12 (2019)
40. S. Bayindir, J. Photoch. Photobio. **372**, 235 (2019)
41. N. Dhanapalan, R. Thangavelu, R.M.M. Ramasamy, J. Appl. Polym. Sci. **129**, 672 (2013)
42. B. Jakimiak, E. Rohm-Rodowald, M. Staniszewska, M. Cieślak, G. Malinowska, A. Kaleta, Rocz. Panstw. Zakl. Hig. **57**, 177 (2006)
43. I.M. Othman, M.A. Gad-Elkareem, K. Aouadi, M. Snoussi, A. Kadri, Org. Chem. Indian J. **4**, 115 (2008)
44. H.F. Rizk, M.A. El-Badawi, S.A. Ibrahim, M.A. El-Borai, J. Korean Chem. Soc. **54**, 737 (2010)
45. H.F. Rizk, M.A. El-Badawi, S.A. Ibrahim, M.A. El-Borai, Arab. J. Chem. **4**, 37 (2011)
46. H.F. Rizk, S.A. Ibrahim, M.A. El-Borai, Arab. J. Chem. **10**, S3303 (2017)
47. M.A. El-Borai, H.F. Rizk, G.B. El-Hefnawy, S.A. Ibrahim, S.S. Aser, H.F. El-Sayed, Fibers Polym. **17**, 729 (2016)
48. V. Patel, M. Patel, R.G. Patel, J. Serb. Chem. Soc. **67**, 727 (2002)
49. N.M. Parekh, K.C. Maheria, Indian J. Fibre Text. Res. **37**, 372 (2012)
50. M.N. El-Nahass, E.A. Bakr, M.M. El-Gamil, S.A. Ibrahim, Appl. Organomet. Chem. **36**, 665 (2022)
51. S.A. Ibrahim, H.F. Rizk, Text. Res. J. **92**, 2849 (2022)
52. M.A. Metwally, M.E. Khalifa, F.A. Amer, Dyes Pigm. **76**, 379 (2008)
53. T.A. Khattab, M.M. Fouda, M.S. Abdelrahman, S.I. Othman, M. Bin-Jumah, M.A. Alqaraawi, H.A. Fassam, A.A. Allam, J. Fluoresc. **29**, 703 (2019)
54. P. Pisitsak, J. Hutakamol, S. Jeenapak, P. Wanmanee, J. Nuammaiphum, R. Thongcharoen, Fibers. Polym. **17**, 560 (2016)
55. M.S. Abdelrahman, S.H. Nassar, H. Mashaly, S. Mahmoud, D. Maamoun, M. El-Sakhawy, T.A. Khattab, S. Kamel, Coatings **10**, 58 (2020)
56. J. Joseph, K. Nagashri, A. Suman, J. Photochem. Photobiol. B. Biol. **162**, 125 (2016)
57. E. Louris, E. Sfiroera, G. Priniotakis, R. Makris, H.E.C. Siemos, I.O.P. Conf, Ser. Mater. Sci. Eng. **459**, 12051 (2018)
58. V.R. Mishra, C.W. Ghanavatkar, N. Sekar, Spectrochim. Acta Part A Mol. Biomol. Spectrosc. **223**, 117353 (2019)
59. H.M. Refat, A.A. Fadda, Eur. J. Med. Chem. **70**, 419 (2013)
60. J. Li, S. Xie, S. Ahmed, F. Wang, Y. Gu, C. Zhang, X. Cha, Y. Wu, J. Cai, G. Cheng, Front. Pharmacol. **8**, 364 (2017)
61. A.I. Seham, F.R. Hala, S.A. Dina, R. Ahmed, Dyes Pigm. **193**, 109504 (2021)
62. J.O. Otutu, E.M. Efurhievwe, J. Appl. Sci. **13**(6), 92 (2013)
63. M. Nakpathom, R. Mongkholrattanasit, Fibers Polym. **21**, 1052 (2020)
64. J. Aguilera, M.V. de Gálvez, C. Sánchez-Roldán, E. Herrera-Ceballos, Photochem. Photobiol. **90**, 1199 (2014)
65. J.T. Lu, E. Ilyas, Cureus. **14**(7), e27333 (2022)
66. G. Cheng, M. Dai, S. Ahmed, H. Hao, X. Wang, Z. Yuan, Front. Microbiol. **7**, 470 (2016)
67. A.M. Ajlouni, I. Mhaidat, W. Al Momani, A.K. Hijazi, Z.A. Tahaa, M. Al Zouby, Jordan J. Chem. **8**, 225 (2013)
68. A. Masri, A. Anwar, N.A. Khan, M.S. Shahbaz, K.M. Khan, S. Shahabuddin, R. Siddiqui, Antibiotics (Basel). **8**(4), 179 (2019)
69. N.M. Boshta, F.A. El-Essawy, M.B. Alshammari, S.G. Noreldein, O.M. Darwesh, Molecules **27**, 3853 (2022)
70. S. Ganguli, M.K. Panigrahi, P. Singh, P.K. Shukla, Int J Pharm Pharm Sci **4**, 434 (2012)
71. S.H. Unnissa, G.K. Reddy, J. Curr, Pharma Res. **3**, 690 (2012)